

DAMAGE EVALUATION OF PRESTRESSED DOUBLE-TEES EXPOSED TO ACCIDENTAL BUILDING FIRE

Brett Tempest, PhD, Dept. of Civil and Environmental Engineering, The University of North Carolina at Charlotte, Charlotte, NC

Matthew Whelan, PhD, Dept. of Civil and Environmental Engineering, The University of North Carolina at Charlotte, Charlotte, NC

ABSTRACT

A concrete masonry building with prestressed double-tee roofing system was damaged in a brief, but intense structural fire. The post-fire examination procedures provided in the PCI document, "Design for Fire Resistance of Precast Prestressed Concrete," were used to evaluate the condition of the roof structure and to determine whether load testing would be justified and safe. This paper presents background on the methods selected for the study and the sampling procedures employed in this particular case. The authors draw correlations between the known location of the fire and damage as determined by visual inspection of the precast units, impact-echo results and Windsor probe results. It was found that the double-tees in areas exposed to the highest temperatures exhibit the greatest in compression wave velocity, and the greatest reduction in concrete compressive strength as indicated by Windsor probe. The results were used to establish the boundaries of fire-related damage to the structure.

Keywords: fire resistance, Windsor probe, impact-echo, damage assessment

INTRODUCTION

One virtue of concrete construction is its native resistance to fire damage as compared with steel and timber construction. Steel and timber have well documented vulnerabilities to fire, which begin impacting strength and elastic characteristics at fairly low temperatures^{1,2}. Reinforced concrete can be easily detailed to withstand the thermal loads associated with structural fires of moderate duration³. However, many prestressed components may exhibit increased susceptibility to fire damage as compared with mild-steel reinforced members due to their lighter section properties and reduced cover requirements. The more economical sections allow the concrete to reach high temperatures more quickly and may offer less protection to the reinforcing materials. Although minimum cover requirements given in ACI 318 are sometimes sufficient to provide code-required fire rating, specific guidance for fire resistant design is not provided in this document⁴. Information specifically related to precast prestressed concrete has been published by PCI⁵.

Expert fire investigators are sometimes able to estimate the temperatures achieved during structural fires. These estimates may provide insight into potential damage sustained by concrete components based on known physical and chemical changes that occur within certain temperature ranges. But given the inherent variability of aggregates, quality of mixing and quality of placing, making such correlations cannot be done with great confidence. In addition, quenching by fluids used to extinguish the fire can significantly aggravate the damage to the concrete. Extensive micro and macro cracking is unavoidable if heated concrete is cooled rapidly.

The evaluation of fire-damaged prestressed concrete structures presents unique challenges due to the impact of heat on the material properties of the concrete and the steel. Exposure to elevated temperatures can induce chemical and physical changes in the concrete that alter strength and elastic characteristics. The case study presented in this paper was undertaken to demonstrate the efficacy of nondestructive testing methods to the condition evaluation of prestressed structural components exposed to fire. The structure being considered was a rectangular, concrete masonry unit bearing wall type building with a prestressed double-tee roof. The building experienced a fire fueled by typical commercial furnishings and wood framing. Design documentation was not available for the 60 year-old structure, therefore the evaluation was conducted by comparing data from two locations in the building, one at the site of the fire and the second away from the fire. Impact-echo readings were collected from a dense grid of points representing a variety of temperature exposure. Additionally, Windsor probes were used to estimate the compressive strength of the concrete. Visual inspection was used to document the location and extent of cracking, spalling, color change, and other damage typical of fire-affected concrete.

IMPACT OF FIRE ON CONCRETE COMPONENTS

The degree of damage to concrete components following fire varies considerably depending on the concrete composition, circumstances surrounding heating duration, maximum temperatures achieved, loading during fire, extinguishing method and rate of cooling. General impacts have been characterized by many researchers investigating

concrete exposed to high temperatures as well as high temperatures accompanied by flames.

Physiochemical changes in the cement paste: At lower temperatures, heat causes water trapped in concrete pores to enter a vapor state. In conditions where the vapor is trapped by an unconnected pore network tensile stresses develop and cause cracks and spalls⁶. As concrete temperatures exceed 200°C, cured cement begins to dehydrate. The loss of bound water is typically complete when temperatures exceed 1,000°C. Hassan et al found substantial reduction of compressive strength in cement cubes heated to temperatures between 200°C and 1,000°C⁷. In addition to strength reduction, dehydration leads to volumetric changes which can cause shrinkage cracking. Further volumetric changes can arise from a form of load induced thermal strain that has been reported by Khoury⁸. This implies that severe thermal conditions in loaded concrete may cause creep-like deformations. Concrete heated under stressed conditions often retains a greater percentage of compressive strength, which is likely due to the restraint against cracking provided by the loading⁹.

Physiochemical changes in aggregate: Elevated temperatures less than 1,000°C most greatly impact the quality of the interfacial transition zone between the cement paste and the aggregate where full breakdown of the bond may occur during heating. The extent of this damage is influenced by aggregate type. Significant alteration in carbonate aggregates is initiated by temperatures above 1,400°C as the aggregate begins to calcine. Siliceous aggregates begin to rapidly lose compressive strength as temperatures surpass 1,000°C. At 1,063°C quartz undergoes crystalline restructuring which is accompanied by volumetric change. Lightweight, expanded aggregates have been the topic of much study related to fire. Conflicting performance observations have been described by Lindgård et al¹⁰. Expanded aggregates seem to exhibit improved fire resistance during lower temperature, cellulose-fueled fires because the aggregates contribute to lower heat conductivity in the concrete. In hotter fires, such as those fueled by hydrocarbon accelerants, the expanded aggregates are characterized by more frequent spalling due to greater moisture content, lower permeability, lower heat conductivity and lower tensile strength.

Much of the chemical alteration coming from exposure of concrete to elevated temperatures is a sole result of heat application. However, the rate of heating and cooling causes thermal shock. Quenching heated concrete specimens with water further aggravates damage mechanically. The impact of the physical and chemical changes described above is manifested at a macro scale in loss of compressive strength, reduction in elastic modulus, failure of bond between mortar and aggregate and failure of bond between concrete and steel.

INVESTIGATING FIRE DAMAGED CONCRETE

In the event of sustained high temperatures, failure of concrete structures during fire is typically the result of loss of flexural capacity, loss of shear capacity, reduction in bond strength, loss of compressive strength or spalling⁸. Due to the inherent fire

resistance of concrete, accidental fires do not often lead to structural collapse. The damage sustained by fire affected structures may be clearly indicated by visually apparent local evidence or by distinct structural deformations. However, the post-fire capacity of components could be hidden by the absence of these visual cues. Or, as may be the case for structures with modular components, the engineer may be responsible for assessing the extent of damage and selecting some components to be replaced and some to remain in service with repairs.

ACI 318 Chapter 20 gives provisions for strength evaluation of existing structures⁴. While the code provides that analytical methods may be used to evaluate structural strength in cases where material properties can be accurately determined, load testing is the only acceptable method when material properties cannot be determined. Fire-type damage renders routine analytical methods difficult to apply for a variety of reasons. The spatial distribution and variation of residual material properties may preclude completing an evaluation with a reasonable number of material samples. The sampling protocol necessary to establish confidence in the test results would be unreasonably burdensome. Further, material tests on discrete materials do not easily confirm the condition of the steel-concrete bond, aggregate-paste bond or the shear capacity of the composite. Therefore, load testing is often the only method that can produce assurance in the soundness of the structure.

The ACI load testing procedure requires application of the larger of the load combinations given in equations (1), (2) or (3) to the structure being tested.

$$1.15D + 1.5L + 0.04(L_r, S, R) \quad (1)$$

$$1.15D + 0.9L + 1.5(L_r, S, R) \quad (2)$$

$$1.3D \quad (3)$$

Where:

D =dead loads

L =live loads

L_r =roof live loads

S = snow loads

R = rain loads

The risk associated with applying loads of such great magnitude to structures with questionable capacity may be too high for routine practice. Increasingly, nondestructive test methods are applied in such cases to satisfy some of the material testing requirements as well as to build confidence in the safety of undertaking a load test. Two nondestructive methods employed in the work described in this paper are impact-echo and Windsor probe, and are described below.

Impact-Echo: This nondestructive evaluation method has been commonly employed to determine the thickness of concrete monoliths as well as to detect voids, internal defects and delamination. Its functioning is based on sensing the reflection of P-waves from the intersection of materials having differing acoustic impedance. Adjacent surfaces, such as

a concrete intersection with air, cause such a reflection. The P-wave travels between reflecting surfaces with a frequency that is related to its propagation speed through the medium as well as the distance between surfaces. An impact-echo evaluation is made by coupling a piezoelectric transducer with the concrete surface and then tapping the surface with an impactor. The transducer records surface displacement as a voltage signal with time. The frequency of the P-wave is found by converting the time domain signal to frequency domain with the Fast Fourier Transform algorithm. P-wave frequency is related to material and component geometry by equation (4).

$$f = \frac{0.96C_p}{2T_m} \quad (4)$$

where:

f = frequency of P-wave speed

C_p = P-wave speed

T_m = thickness of test member

Manipulation of Equation (4) for purposes of determining thickness monolithic materials is a simple task. Discovering changes in material characteristics requires consideration of factors which predict the P-wave velocity, C_p . This quantity is taken as

$$C_p = \sqrt{\frac{E(1-\nu)}{\rho(1+\nu)(1-2\nu)}} \quad (5)$$

where:

E = modulus of elasticity

ρ = material density

ν = Poisson's ratio

The influence of heat damage to concrete is likely to alter the elastic modulus of the material, Poisson's ratio and material density. However, holding other variables constant, values of ν between 0.10 and 0.30, affect C_p by -4% and +10% respectively with comparison to the accepted value of $\nu=0.20$ for concrete. Such small variation in test results would not be notable given other variables typical of concrete construction. Similarly, because of dehydration, aggregate expansion and restructuring of the pore network, heat treated concrete would be assumed to decrease in density. Since C_p is inversely proportional to ρ , it is conservative to hold ρ constant for analysis since it would likely actually be lowered during a fire. Conversely, the magnitude of anticipated changes in the elastic modulus, E , would create significant changes in C_p . Therefore, the fundamental assumption of investigators using impact-echo methods for fire damage detection is that compromised concrete will exhibit lowered C_p , which is associated with reductions in modulus of elasticity and with reduced component capacity.

Windsor probe: A second method employed in the evaluation of fire-damaged concrete is the Windsor probe. Penetration methods, such as Windsor probe, are based on empirical relationships between the depth to which a probe or pin enters a concrete matrix when launched at the surface with a known velocity or pushed in with a known force¹¹. In the Windsor probe method described by ASTM C803, a probe is propelled into the concrete via a charge fired from a gun-like device. The penetration depth is determined by measuring the portion of the probe remaining outside the concrete and subtracting it from the overall length of the probe before the test. Typically three probes are set and an average of the penetration depths is used to render a concrete strength estimate.

As the probe enters the concrete, it is driven through both cement mortar and aggregates. Whereas the aggregate properties usually have a diminished impact on the compressive strength of concrete, it can have a significant impact on the penetration depth of the probe. Therefore, results are typically adjusted based on the Moh's hardness of the aggregate.

CASE STUDY

A concrete masonry building with prestressed double-tee joist roof in North Carolina was subjected to a brief, accidental fire. Although the duration of the fire was short, the combination of intense heat and extinguishing methods contributed to visibly apparent damage of the joists. Decisions for how to proceed with building restoration or reconstruction required reliable determination of the extent of the damage. Poor access to the top surface of the double-tees, the visual appearance of damage and the unknown condition of the CMU walls presented too much risk to safely undertake a load test without additional information that could be used to build confidence in the capacity of the structure. Nondestructive methods were selected to locate the extent of the fire damage and to formulate recommendations regarding appropriateness of a load testing exercise.

The roof plan of the building was rectangular with length of 135' and width of 54' as shown in Figure 1. There were a total of 33 double-tee joists which spanned between the outer CMU bearing walls. The joists referenced in this paper are labeled from A through J, with A being the unit closest to the north wall of the facility. Cross-section details of the joists are shown in Figure 2. Although there was no design documentation available, the investigators assumed values in Table 1 as typical for double-tee units contemporary with the building. Initial visual inspection of the joists led the team to suspect damage in the northernmost 10 joists which were closest to the known location of the blaze. Heat-sensitive materials such as plastic containers, carpet, and paper were found in-tact towards the southernmost portion of the building, leading the investigators to assume that the joists in this area were also undamaged.

There was not an opportunity to collect and destructively test materials. Instead, the team made baseline measurements in the area of the facility that was not exposed to fire for comparison. Windsor probes, impact echo and visual inspection techniques were used to map damage to the roof structure and to prepare estimates of material deterioration due to heat and fire exposure. The team was able to access the underside of the double-tees by erecting scaffolding that provided access to the fire affected zone as well as the baseline area.

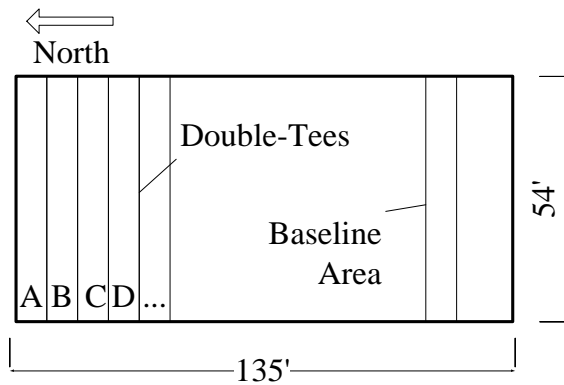


Figure 1 Building layout

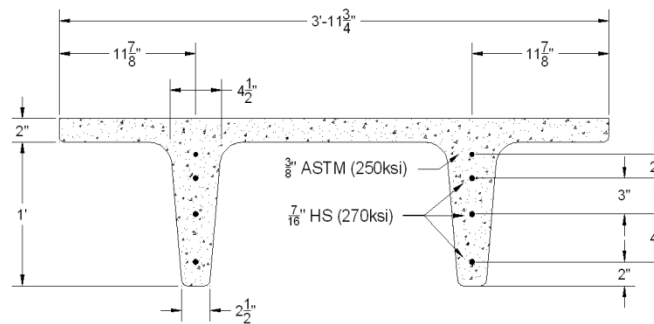


Figure 2 Double-tee cross-sectional profile

Table 1 As-built material properties typical of double-tee joists

Concrete Properties			
Unit Weight	120 pcf	Cement	C150
Compressive Strength, f_c	5,000 psi	Aggregate	C33 or C330
Reinforcing Steel Properties			
Reinforcing Steel	A615 or A305	Welded Wire Fabric	A185
WWR Tensile Strength		75 ksi	
Prestressing Strand Properties			
ASTM Grade Ultimate Strength	250 ksi	HS Grade Ultimate Strength	270 ksi

Windsor probes were set in the baseline joist and joists B, D, G and I. The team fired three probes at each location and used the average penetration depth to predict concrete strength with correlation data provided by the instrument manufacturer. Moh’s hardness of the aggregates was measured using several pieces of exposed aggregate in the concrete. The aggregate appeared to be an expanded, lightweight material and showed hardness values between 3 and 7. Because of the inherent variability in lightweight aggregate hardness, an average value of 5 was used for strength estimation purposes. Table 2 summarizes the findings of the Windsor probe investigation.

Table 2 Windsor probe results

Stem Label	Average Probe Depth [inches]	Estimated Strength Using Moh's Hardness of 5 [psi]	% Difference from Baseline
B1	1.41	3,915	46.5
D2	1.37	4,220	42.3
G1	1.19	5,530	24.5
I2	1.06	6,490	11.3
Baseline	0.91	7,320	-

Impact-echo test sites were located 5” from the base of the double-tee stem and distributed at 12” intervals along the length of both stems of the joists under study. In all, 52 points were sampled of each double-tee stem, or 104 for each double-tee unit. Impact-echo test sites were located on the flange at 24” intervals along the length of each unit. Collected data consisted of a displacement time series which was processed to isolate the frequency of the P-wave. Table 3 presents a summary of the data, which includes the lowest frequency value measured along the length of each stem as well as the average of all values found along the stem. The average frequency found in the baseline specimens was approximately 21 kHz. For comparison, the lowest flange frequencies are also presented in Table 3, however these show much less variability from unit to unit. Stems closest to the fire location (B,C,D & E) presented relatively lower average frequencies, which were sometimes less than half the value of the baseline area. Applying the assessment that the elastic modulus, E , of the concrete is the term in equation (5) that would produce significant changes in the value of C_p , it is presumed that frequency values presented in Table 3 reflect a decrease in elastic modulus that is associated with fire damage.

Combining equations (4) and (5) and solving for E , the frequency determined by Impact- Echo was used to estimate the elastic modulus of the concrete. These estimates are presented in the rightmost column of Table 3. The modulus of elasticity computation yielded values of approximately 3,000,000 psi for the undamaged material in the baseline area. This value is reasonable for lightweight aggregate concrete having unit weight of 120 pcf and f'_c between 4,000 and 5,000 psi. It should be noted that in the fire affected areas, the modulus of elasticity estimated from the average frequency in the most damaged joists was found to be less than 50% of the baseline value. This would indicate seriously compromised material properties as well as markedly reduced joist stiffness.

The findings of the two quantitative nondestructive test methods were corroborated by observations made during visual inspection of all joists located in the test area. Typical damage that was cataloged consisted of crazing, cracks, spalls, and delamination, as shown in Figures 3 and 4. The team located cracks ranging in width from 0.005” to 0.06”. Spalling was found on several of the joists and often exposed steel mesh as well as prestressing strands. Figure 5 provides a spatial mapping of the damage discovered during the visual inspection. The fire location is within the circle plotted on Figure 5. Cracking and spalling is evident on joist locations within approximately 30’ of

the fire. The most severe damage was located on joists B, C and D, directly over the fire location.

The visual inspection included measurement of change in camber by surveying the elevation of the stem bottoms along the length of several units. Measurements were made at 0, 10, 20, 30, 40, 50, and 53 feet from the west wall. The results are presented in the Figure 6, in which the circles represent the surveyed value measured relative to the beam end and the solid line represents the predicted camber profile for an undamaged beam. It can be seen that stem B2, C1 and C2 show marked loss of camber while stems D1, D2 and E1 show camber gains.

Table 3 Impact-Echo results from stems and flanges

Joist and Stem	Minimum Frequency Measured in Stems [kHz]	Average Frequency Measured in Stems [kHz]	Minimum Frequency Measured in Flange [kHz]	% Difference in Stems Relative to Baseline	Estimated Modulus of Elasticity Based on Stems [psi]
Baseline1	19.2	20.8	22.7	NA	2,935,370
Baseline2	17.6	21.0		NA	2,998,958
A1	14.2	17.8	22.0	-14.8%	2,159,289
A2	12.5	17.6		-15.8%	2,111,901
B1	10.8	16.4	21.3	-21.5%	1,817,092
B2	7.4	15.1		-27.8%	1,817,092
C1	8.4	14.5	21.8	-30.6%	1,426,307
C2	9.5	14.7		-29.7%	1,462,128
D1	7.8	13.5	22.3	-35.4%	1,227,144
D2	9.3	14.3		-31.6%	1,408,318
E1	10.2	15.3	26.3	-26.8%	1,599,983
E2	11.2	16.4		-21.5%	1,837,242
F1	12.3	16.6	22.7	-20.6%	1,867,470
F2	10.3	16.6		-20.6%	1,870,139
G1	14.3	16.9	26.3	-19.1%	1,941,280
G2	13.3	16.8		-19.6%	1,924,812
H1	15.1	17.3	22.7	-17.2%	2,043,527
H2	15.3	17.6		-15.8%	2,117,067
I1	14.9	18.0	25.8	-13.9%	2,212,780
I2	15.3	18.2		-12.9%	2,244,676
J1	14.5	18.4	21.7	-12.0%	2,300,142
J2	14.1	18.2		-12.9%	2,252,490



Figure 3 Spall and exposed prestressing strand



Figure 4 Cracking near location of prestressing strand

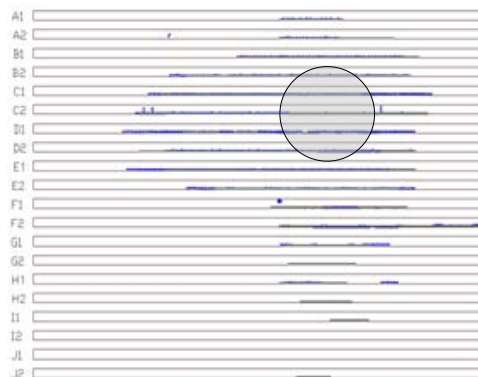


Figure 5 Location of damage discovered by visual inspection

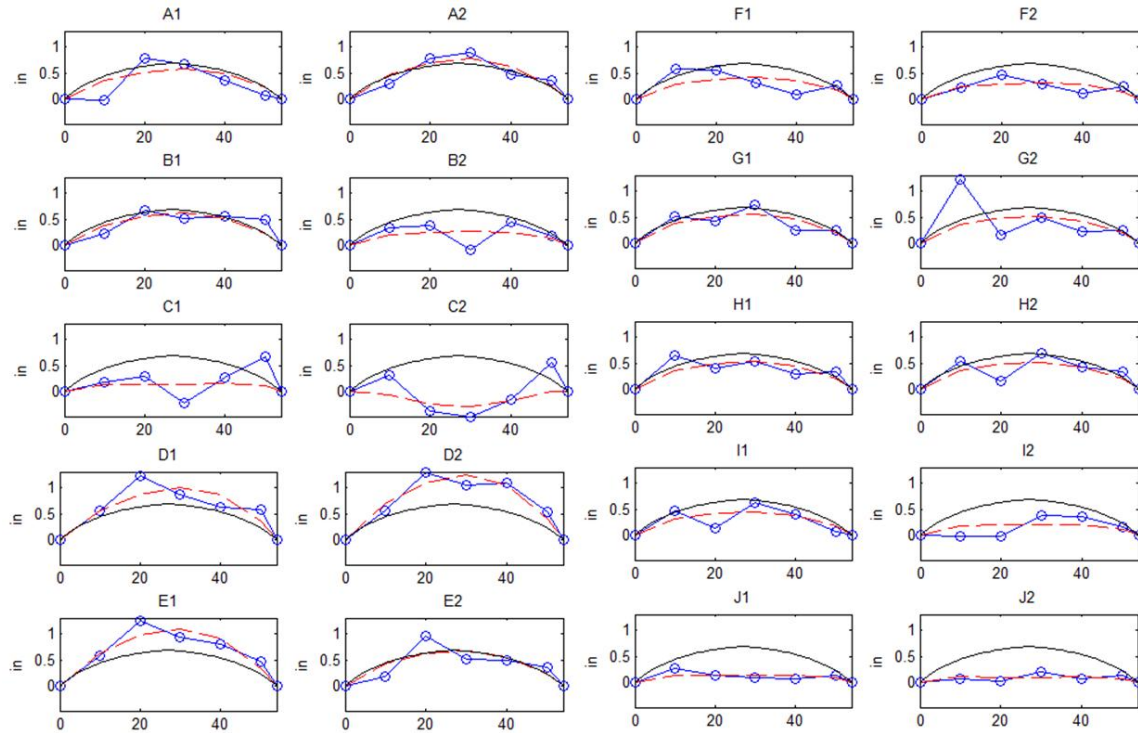


Figure 6 Camber measurements of units A through J

INTERPRETATION OF TEST RESULTS

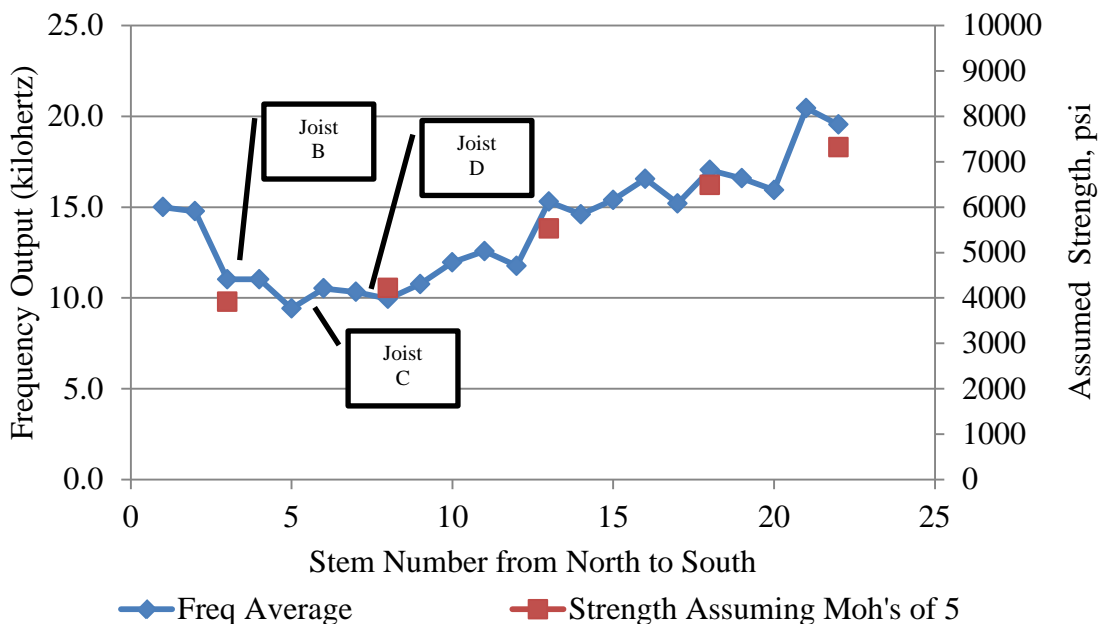
The three inspection methods used to ascertain the degree of fire-induced damage to the roof joist system were uniform in indicating the most significant material changes closest to the known location of the blaze. The results of the methods described indicate that the fire has caused substantial changes in the capacity of the roof system. Windsor probe data predicts a 46.5% reduction in concrete compressive strength in unit B stems as compared to the baseline. This change in strength is sufficiently large to warrant concern that the joist could easily become overloaded during normal service. Impact-echo results predict a 58.6% decrease in elastic modulus from 2,998,958 psi in the baseline area to 1,227,144 psi in unit D. This change in material characteristics is sufficient to cause considerably reduced stiffness and potential for greater deformations. Such deformations were indicated by increased camber in unit D. In addition to concern over excessive deflections and global failure, the threat of local failures in the most compromised portions of the units presents hazards from falling debris.

Table 3 also gives a comparison of the P-wave frequency measured by impact echo in the flanges versus the stems. The flange frequencies are not notably changed relative to the baseline. This may indicate that either the stems became hotter than the flanges during the fire or that they were more damaged by quenching during fire fighting. When this information is taken in together with change in camber measurements, some speculation about the nature of damage to the prestressing steel is possible. Because there was no significant variation in flange concrete modulus of elasticity, it appears that the joists that gained in camber possibly did so due to decreased concrete modulus of elasticity. Conversely, the joists that lost camber (B and C) possibly did so following loss of prestress due to loss of strand bond or heat damage to the steel.

It is apparent that the joists displaying the most visually obvious damage (as depicted in Figure 7) are associated with the largest quantified changes in material behavior. Joists B, C and D were identified as the most impacted by Windsor probe data and impact-echo data. These were also the joists with the most extensive visual damage and change in camber. In the case of joists F and G, there was not alarming visually apparent damage. However, the impact echo and Windsor probe data predict reductions in elastic modulus and compressive strength of nearly 30%. In these cases, nondestructive tests were necessary to locate the damage not appreciable by eye.

In the absence of companion data from destructive tests, the results are not calibrated. However the impact-echo results and the Windsor probe results have illustrated a similar trend towards lower modulus of elasticity and lower compressive strength respectively. The magnitude of these changes is similar and the data are plotted simultaneously in Figure 7. The impact-echo data shown in Figure 6 consists of readings taken at the same location as the Windsor probes were set, so they are representative of the same material and damage conditions.

Figure 7 Correlation of Windsor probe and impact-echo findings



CONCLUSIONS

Nondestructive test methods were used to complete an efficient investigation of a fire-damaged building with prestressed double-tee joist roof system. Impact-echo and Windsor probe methods were used to describe condition of joist units which were exposed to fire in comparison to units which were not exposed. Reductions in strength and elastic modulus of 40-60% were discovered by both methods with very good agreement in the location of the most heavily damaged units. The methods were able to detect changes in material consistency that were not obvious through visual inspection.

The impact-echo method was particularly efficient in generating a dense grid of data. The Windsor probe method would be a cumbersome alternative for creating as dense a damage map because of the time required to complete each sample and the expense of each charge. Also, the probes cause significant surface damage that would be objectionable if it were widespread. Operator training for impact-echo evaluation is more difficult due to the complexity of the methods. Without companion data from destructive tests, the nondestructive methods do not provide exacting estimates of strength and elastic material properties. However, they do provide sufficient evidence that the damage sustained by the joists B, C, D and E renders them unsafe. Load testing in this area of the building would not have been possible without exposing the evaluators to great risk as well as potentially causing additional damage to the building.

REFERENCES

1. Breyer, D. E. (2003). Design of wood structures--ASD. New York, McGraw-Hill.
2. McCormac, J. C. (1981). Structural steel design. New York, Harper & Row.
3. MacGregor, J., Wight, J.. Reinforced concrete : mechanics and design. 2005 Englewood Cliffs, N.J., Prentice Hall.
4. American Concrete Institute. Building code requirements for structural concrete : (ACI 318-08) and commentary (ACI 318R-08), 2008, American Concrete Institute.
5. Gustaferro, A., Martin, L., Design for fire resistance of precast prestressed concrete. 1989, Chicago, IL, Prestressed Concrete Institute.
6. Gosain, N., Drexler, R., Choudhuri, D. "Evaluation and Repair of Fire-Damaged Buildings," *Structure*, Sept. 2008, 18-22.
7. Hassaan, M., Salah, S., Eissa, N. "Study of the dehydration of Portland Cement by Mössbauer spectrometry" *Hyperfine Interactions* V. 46, No. 1 March 1989, 733-738.
8. Khoury, G. Grainger, B, Sullivan, P. Strain of concrete during first heating to 600°C under load, *Magazine of Concrete Research* V. 37, No. 133 1985, 195–215.
9. Petkovski, M.. "Effects of stress during heating on strength and stiffness of concrete at elevated temperature." *Cement and Concrete Research* V.40, No.12, Aug. 2010, 1744-1755.
10. Lindgård, J., Hammer, T. Concrete—A Literature Survey with Focus on Spalling, Supplementary Papers, Fourth CANMET/ACI/JCI International Conference on Recent Advances in Concrete Technology, Tokushima, Japan 1998, 25–39
11. American Concrete Institute. ACI manual of concrete practice. 2003, American Concrete Institute.